A Parallel Connected Unfolding Bridge (PCUB) Multilevel Converter for HVDC Applications

Zain Hassan, Alessandro Costabeber, Francesco Tardelli, Alan Watson and Jon Clare
University of Nottingham
Nottingham, UK
zain.hassan@nottingham.ac.uk

***Abstract*—Hybrid Voltage Source Converters (VSC), that combine the conventional three-level VSCs and Modular Multilevel Chain-Links (CLs), offer a promising solution for future HVDC stations, achieving reduced footprint with respect to the MMC while maintaining high power quality and low loss. This paper introduces a new hybrid solution named 'Parallel Connected Unfolding Bridge Modular Multilevel Converter' (PCUB) which uses a parallel connection of phases on the DC side and comprises of wave shaping Chain-Links and unfolding H-bridges. This paper presents the operating principle and basic mathematical model of the PCUB and also details an optimisation of the transformers turn ratio for the minimisation of the energy requirements in the CLs. PLECS simulation results for the proposed topology operating at 20kV DC - 11kV AC and 20MW are also presented to demonstrate its performance.**

***Index Terms*—HVDC, power conversion, multilevel converter, modular converter.**

I. Introduction

High-Voltage Direct Current (HVDC) can be used to transmit bulk power over long distances where it proves more cost-effective than AC transmission because of the lower transmission losses [1]. This includes transmitting power from remote electricity sources such as off-shore wind power stations, and for interconnection of grids between countries.

Power electronics technologies have gained an ever-growing role in power systems over the last few decades. Controllable semiconductor devices such as thyristors and transistors are in use since the 1970s and are the technologies of choice for high-power systems because of their fast switching and high current-carrying capability [4]. Conventional HVDC systems use Line-Commutated Converters whereas in the recent years, Voltage-Source Converters (VSCs) which usually employ IGBTs have taken over due to their benefits over LCC-HVDC [2], [3] such as better performance in weak AC grid conditions, low harmonic content and the ability to control real and reactive power independently [5].

The earlier topologies used in the VSC-HVDC were two-level and three-level converters [6] [7]. Their main limitations where high switching losses, limited number of voltage levels and inadequate DC-side fault behaviour [8]. These have been overcome by the Modular Multilevel Converter (MMC) introduced in 2001 by Marquardt [7]. Employing a modular approach where identical half-bridge or full-bridge submodules are stacked in series, this converter is easily scalable to any voltage level and results in waveforms with negligible harmonic content [5]. Since each submodule is switched in and out only once in the full voltage period, the switching frequency is effectively reduced to the fundamental frequency resulting in low switching losses [6]. Owing to its modularity that allows it to meet any voltage requirement, low switching losses that enhance its efficiency and low harmonic content that significantly reduce the filtering requirements [9] [10], the MMC has gained considerable recognition in VSC-HVDC and has been employed by the industry in commercial HVDC projects.

In order to further develop the technology and improve some of the aspects of the MMC, several other hybrid VSC topologies have been proposed in literature that have the characteristics of both two-level and multilevel converters. The Alternate Arm Converter (AAC) was proposed in [11] that provides DC fault blocking capability without any compromise on the efficiency. The AAC has almost a similar structure to the MMC except for director switches in the upper and lower arms and the use of full-bridges as submodules [12]. Another hybrid multilevel converter topology is the Series Bridge Converter (SBC) proposed in [13] with series connection of converter phases on the DC side. The SBC topology has the benefit of a significantly more compact footprint than the MMC but the drawback of a limited power transfer capability during AC faults, due to the constraints imposed by the series connection of phases on the DC side.

In this paper, the PCUB, a new hybrid VSC topology is introduced in order to overcome the drawbacks of the SBC [13] while maintaining smaller station footprint than the MMC because of the need for smaller sub-module capacitors in the chainlinks. During the design stage, this is achieved by setting the AC side transformer turn ratio to an optimum value that minimises the energy storage requirements of the converter. For the sake of brevity, the analysis of the operating principle of the converter is discussed under balanced grid conditions and validated with a full switching simulation model in PLECS that confirms the theoretical claims.

II. Converter Topology

Figure 1 shows the PCUB topology. In each AC phase it employs a conventional H-bridge converter along with wave shaping CLs and hence belongs to the hybrid VSCs. Like the MMC and the AAC, the three converter phases in the PCUB are connected in parallel across the DC side. Each

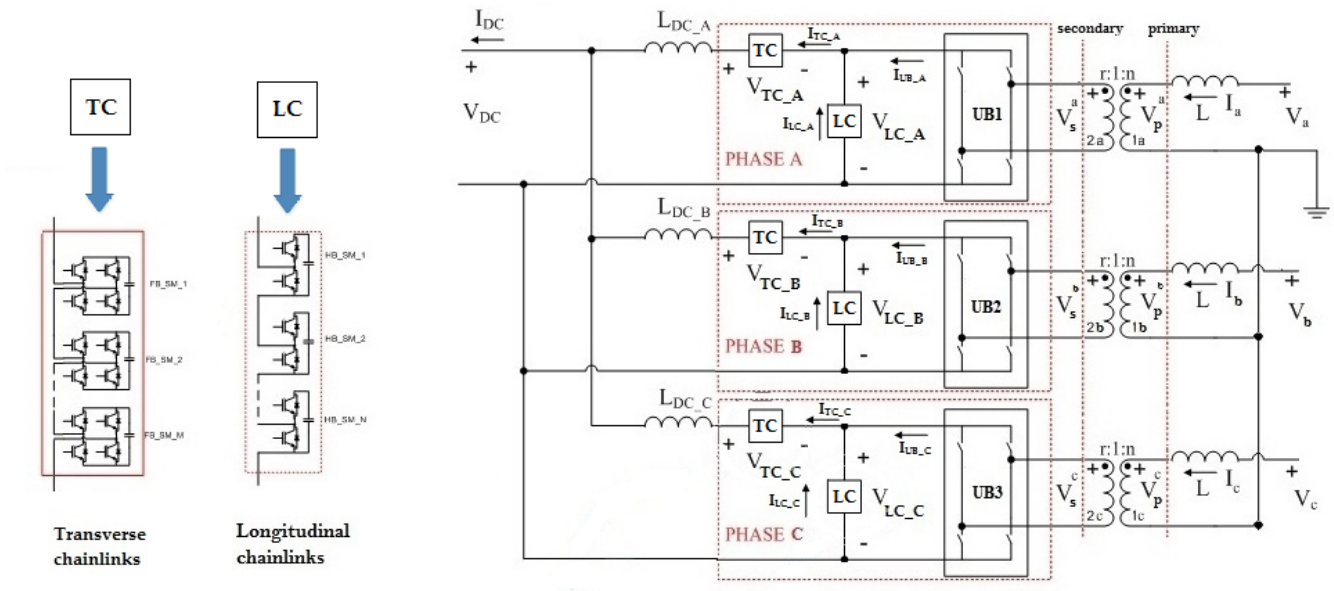

Fig. 1. Proposed converter topology

phase consists of a DC-side phase reactor, two CL arms and a soft-switched Unfolding Bridge (UB) which is interfaced to the AC network through a transformer. Each of the switches in the UB is formed by a string of IGBTs. The shunt-connected Chain-Links, named *Longitudinal Chainlinks* (LC), are made of half-bridge submodules (SM) and the series connected Chain-Links, named *Transverse Chainlinks* (TC), are made of full-bridge SM. The LCs synthesise a full wave rectified multilevel voltage waveform, the amplitude of which is imposed by the AC side P-Q operating point. This rectified multilevel waveform is unfolded by the H-bridge (UB) at the zero crossings to generate the AC side voltage. Because of the imposition of the LC voltage by the AC side and due to it being a rectified waveform, this voltage has an average component and even harmonics, all of which have amplitudes depending on the AC side operating point. Hence, the TC voltage waveform is synthesised in such a way that all the AC components in the LC are cancelled out on the DC side of each phase. It is worth mentioning that other waveshaping solutions are possible but the paper will focus on the full AC cancellation for simplicity.

III. Mathematical Analysis

To understand the basic operation and waveshaping of the CLs in the PCUB and to facilitate a design optimisation process, it is helpful to derive mathematically the instantaneous expressions of voltages, currents and power/energy in the converter CLs. In order to keep the analysis simple, the CLs are considered symmetrical and lossless. They are treated as controllable voltage sources and the effects of switching are neglected. Under ideal grid conditions, each phase needs to generate a target phase voltage expressed in (1).

$$V_k = V\sin(\omega t - k\frac{2\pi}{3}) \tag{1}$$

where $k \in (a, b, c)$ for phases a, b and c respectively and V is the grid voltage amplitude. In order to simplify the analysis, only phase a is considered and thus the AC side voltage and currents can be described by (2)

$$\begin{aligned} V_a &= V\sin(\omega t) \\ I_a &= I\sin(\omega t + \phi) \end{aligned} \tag{2}$$

An arbitrary turn ratio value r is assumed for the AC transformer to allow its optimisation. Therefore, the voltage and current on the transformer secondary are given by (3) (reference to phase 'a' is omitted for brevity)

$$\begin{aligned} V_s &= rV\sin(\omega t) \\ I_s &= \frac{I}{r}\sin(\omega t + \phi) \end{aligned} \tag{3}$$

The instantaneous voltage that the LC should synthesise is a full-wave rectification of the AC voltage on the transformer secondary and is expressed as:

$$V_{LC}(t) = rV|\sin(\omega t)| \tag{4}$$

The instantaneous voltage to be synthesised by the TC is the difference between V_{DC} and V_{LC} and is given as:

$$V_{TC} = V_{DC} - rV|\sin(\omega t)| \tag{5}$$

Fourier series expressions for (4) and (5) are computed to define the harmonics and are presented in (6) and (7):

$$V_{LC}(t) = \frac{2rV}{\pi} - \frac{4rV}{\pi}\sum_{n=2,4,6\ldots}^{\infty}\frac{1}{n^2-1}\cos(n\omega t) \tag{6}$$

$$V_{TC}(t) = V_{DC} - \frac{2rV}{\pi} + \frac{4rV}{\pi}\sum_{n=2,4,6\ldots}^{\infty}\frac{1}{n^2-1}\cos(n\omega t) \quad (7)$$

From (6) and (7), it is observed that both the CL voltages are formed of DC terms and even harmonics of decaying amplitudes.

Due to the parallel connection of converter phases on the DC side, one-third of the DC current flows in each phase. Since the TC is meant to cancel out all the AC voltage components in the LC, only DC current flows in TC. Because of the unfolding action, the current at the input of UB I_{UB} is the full-wave rectification of the AC current on the transformer secondary with the required phase-shift in case of reactive power flow. Current through the LC is then the difference between I_{UB} and TC current. All currents and their Fourier series expressions are given in (8)-(10):

$$I_{LC}(t) = \begin{cases} \frac{I}{r}|\sin(\omega t+\phi)| - \frac{I_{DC}}{3} & 0 \le t \le \frac{\pi}{\omega} \\ -\frac{I}{r}|\sin(\omega t+\phi)| - \frac{I_{DC}}{3} & \frac{-\pi}{\omega} \le t \le 0 \end{cases} \quad (8)$$

$$I_{LC}(t) = \frac{I}{r}\left[\frac{2}{\pi}\cos\phi - \frac{4}{\pi}\cos\phi\sum_{n=2,4,6\ldots}^{\infty}\frac{1}{n^2-1}\cos(n\omega t) + \frac{4}{\pi}\sin\phi\sum_{n=2,4,6\ldots}^{\infty}\frac{n}{n^2-1}\sin(n\omega t)\right] - \frac{I_{DC}}{3} \quad (9)$$

$$I_{TC} = \frac{I_{DC}}{3} \quad (10)$$

IV. Power Balance and Second Harmonic Injection

For successful operation of a multilevel VSC converter, one of the necessary conditions is that there is no average power dissipation in the chainlinks. Although there are fluctuations in the amount of charge in the submodule capacitors over time because of the AC current flowing through them, it is imperative to maintain this charge close to a nominal value. This is achieved by ensuring that the average power in the individual chainlinks is zero over a period.

Unlike the MMC, the average power in the individual chainlinks in the PCUB is not inherently zero with the intuitive waveshaping discussed so far, because of the full-wave rectification stage at the UB which causes DC and even harmonics to flow inside the converter chainlinks. CL voltage and current expressions in (6)-(10) are used to get the mean power expressions in the LC and the TC.

$$\begin{aligned} \bar{P}_{LC} &= \frac{rV^2I}{\pi V_{DC}}\cos\phi - \frac{VI}{2}\cos\phi \\ \bar{P}_{TC} &= -\frac{rV^2I}{\pi V_{DC}}\cos\phi + \frac{VI}{2}\cos\phi \end{aligned} \quad (11)$$

It can be observed that the mean powers in both chainlinks are equal and opposite. Hence,

$$\bar{P}_{LC} = -\bar{P}_{TC} \quad (12)$$

Therefore, to ensure power balance, power needs to be 'moved' from one CL to the other in each phase until both mean powers are zero. This is achieved by modifying the waveshaping in order to add a control variable that can be used for balancing. Observing that the even harmonic components in the LC and the TC voltages in (6) and (7) are in phase opposition, the presence of even harmonic currents through both CLs would dissipate equal and opposite mean powers in them, achieving the desired effect. For the PCUB, only the injection of second harmonic current, $i_{2\omega}$ in the CLs is proposed.

The 2ω current that needs to be injected is either in phase or in anti-phase with the 2ω voltage components in the CLs depending on the direction of power flow. Since V_{LC} is imposed by the AC side and no additions can be made to it, $i_{2\omega}$ is driven by adding 2ω components only in V_{TC} as shown in (13).

$$V_{TC}(t) = V_{DC} - \frac{2rV}{\pi} + \frac{4rV}{\pi}\sum_{n=2,4,6\ldots}^{\infty}\frac{1}{n^2-1}\cos(n\omega t) + \boldsymbol{k\sin(2\omega t)} \quad (13)$$

where k is the 2nd harmonic gain. The DC side voltage equation after the addition of 2nd harmonic is:

$$(V_{LC}+V_{TC}) - V_{DC} = L_{DC}\frac{di_{2\omega}}{dt}$$
$$k\sin(2\omega t) = L_{DC}\frac{di_{2\omega}}{dt}$$

$$i_{2\omega} = -\frac{k}{2\omega L_{DC}}\cos(2\omega t) \quad (14)$$

Thus, a 2ω current is forced through the DC reactor of each phase, introducing opposite and equal mean power components in the LC and the TC. The power components added due to the 2ω current are highlighted in bold.

$$\begin{aligned} \bar{P}_{LC} &= \frac{rV^2I}{\pi V_{dc}}\cos\phi - \frac{VI}{2}\cos\phi - \boldsymbol{\frac{rkV}{3\pi\omega L_{DC}}} \\ \bar{P}_{TC} &= -\frac{rV^2I}{\pi V_{dc}}\cos\phi + \frac{VI}{2}\cos\phi + \boldsymbol{\frac{rkV}{3\pi\omega L_{DC}}} \end{aligned} \quad (15)$$

From (15), an expression for 2nd harmonic gain k can be found for the goal of driving mean chainlink powers to zero which is shown in (16). The expression shows a dependence of k on the DC reactor value and the AC operating point, showing that in practical implementation k will be driven by a dedicated energy balancing controller.

$$k = 3\omega L_{DC} I\cos\phi\left(\frac{V}{V_{DC}} - \frac{\pi}{2r}\right) \quad (16)$$

The current in the LC and the TC, after taking into account the circulating current, can be expressed as:

$$I_{LC}(t) = \frac{I}{r}\left[\frac{2}{\pi}\cos\phi - \frac{4}{\pi}\cos\phi \sum_{n=2,4,6\ldots}^{\infty} \frac{1}{n^2-1}\cos(n\omega t) + \frac{4}{\pi}\sin\phi \sum_{n=2,4,6\ldots}^{\infty} \frac{n}{n^2-1}\sin(n\omega t)\right] - \frac{I_{DC}}{3} - \frac{k}{2\omega L_{DC}}\cos(2\omega t) \quad (17)$$

$$I_{TC}(t) = \frac{I_{DC}}{3} - \frac{k}{2\omega L_{DC}}\cos(2\omega t) \quad (18)$$

V. Turn Ratio Optimisation

Since the PCUB uses a two-level H-bridge arrangement in conjunction with multilevel CLs, the effect of turn ratio on sizing and energy requirements of the CL is not straightforward. In this paper, a design of the turn ratio is proposed for the converter based on minimisation of energy requirements in the CLs. The transformer arrangement in Figure 1 has its primary connected to the AC side and secondary connected to the unfolding bridges and the turn ratio from primary to secondary is 1:r.

TABLE I
System Ratings for Turn Ratio Analysis

System Parameter	*Rating*
Active Power P	± 20 MW
Reactive Power Q	± 8 MVAr
AC Voltage V_{l-l}	11 kV
DC voltage	20 kV

System ratings for the turn ratio analysis are given in Table I. To conduct this analysis, instantaneous energy expressions for the chainlinks are first evaluated by integrating the product of (6) and (17) for the LC and the product of (13) and (18) for the TC. CL energy expressions are then used in a Matlab script to calculate worst-case peak-to-peak energy pulsation in the chainlinks for the given system ratings for different turn ratio values. Worst-case means that the complete P-Q operating region is swept for each turn ratio to find the most demanding energy pulsation values. The required SM capacitance values in the CLs is then calculated from the peak-peak energy pulsation for every turn ratio value using the following expression:

$$C_{cell} = \frac{\triangle E}{\rho_{pk-pk} n V_{cell}^2} \quad (19)$$

where

- $\triangle E$ is the peak-peak energy pulsation
- ρ_{pk-pk} is the peak-to-peak ripple factor taken as 20%
- V_{cell} is the nominal cell voltage of 1.5 kV
- n is the number of submodules which changes with the turn ratio value and is repeatedly calculated for every data point by dividing the worst-case voltage pulsation in the CLs by V_{cell}

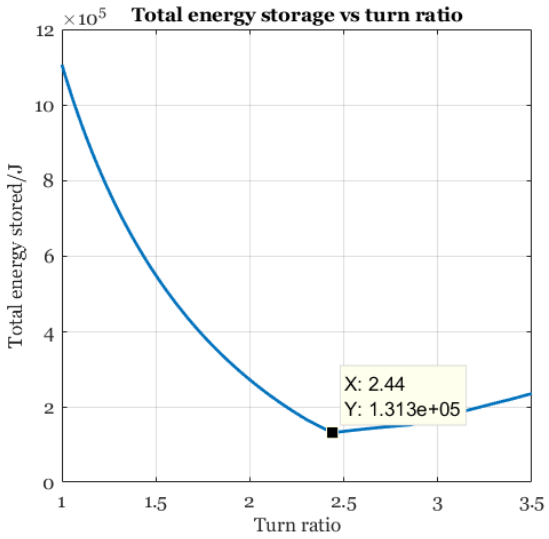

Fig. 2. Worst-case energy storage for changing turn ratio

Total energy stored in the converter CLs (all 3 phases) is then calculated as:

$$E_{stored} = 3 * \left(\frac{1}{2} n_{LC} C_{LC} V_{cell}^2 + \frac{1}{2} n_{TC} C_{TC} V_{cell}^2\right) \quad (20)$$

where C_{LC} and C_{TC} are the SM capacitances and n_{LC} and n_{TC} are the number of SMs required.

E_{stored} is then plotted for a range of turn ratio values. The results of the analysis are presented in Figure 2. From the results, it can be seen that the overall energy storage of both CLs is minimised for a turn ratio value of 2.44.

Unit Capacitance Constant (UCC) [15], also known as H constant, time constant or energy storage (referred to as 'energy storage' in this paper), is a unified constant which is a measure of the energy stored in the converter per unit of rated power and can be used as a rough comparsion of the sizes of different multilevel converters. Assuming operation at the optimum turn ratio value, E_{stored} in the converter is 131.3 kJ and the energy storage is calculated as:

$$\textit{Energy storage} = \frac{E_{stored}}{P} = \frac{131.3kJ}{20MW} = 6.6ms \quad (21)$$

The energy storage for PCUB is 6-7 times smaller than the energy storage for MMC found in literature that is between 40 ms and 50 ms [16] [17]. Hence, the PCUB can be said to have a much smaller footprint than the MMC.

VI. Control Strategy

Due to the parallel connection of phases on the DC side, each phase in the PCUB can be controlled independently. This makes it possible to design the control scheme for single phase and extend the same scheme to the other two phases. The control loops needed in the PCUB are:

- AC current

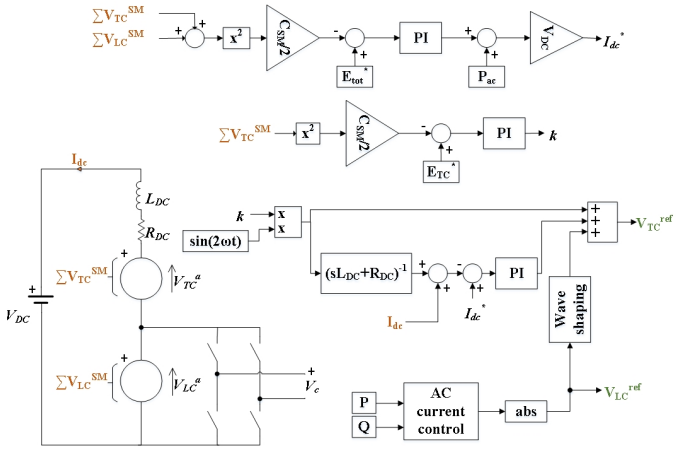

Fig. 3. Control scheme for PCUB

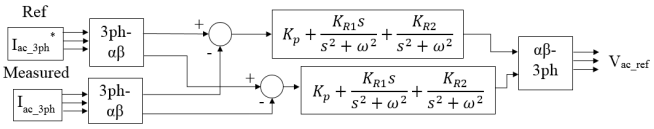

Fig. 4. AC current control block diagram

- DC side current
- Total converter energy per phase
- Inter-arm energy management between LC and TC

Please note that additional loops are required to deal with unbalanced and faulty operation, not discussed here for brevity. Proportional-Integral (PI) controllers are used for DC current, total energy and inter-arm energy control and Proportional-Resonant (PR) controller is used for AC current control. A block diagram of the control scheme of a single phase of the PCUB is shown in Figure 3, where it is assumed that AC active and reactive power demands are imposed by the grid operator and the DC power can be controlled. The first control objective is to maintain the total energy in the CL arms, keeping the SM capacitors at nominal V_{cell}. Hence, the total energy loop generates the current reference for the inner DC current control loop. The output of the DC control loop is the reference signal for the modulator which produces gating signals for the TC only since the mean voltage in the LC is imposed by the AC side current control. The inter-arm energy management control ensures that a uniform energy distribution between the LC and the TC is maintained in each phase. This is achieved by controlling the gain of the 2nd harmonic component added to the TC voltage. In order to decouple the DC current controller and the inter-arm energy management controller, the 2ω circulating current needs to be subtracted from the measured current on the DC side of each phase.

On the AC side, a decoupled current control loop ensures the required power flow by controlling the AC current. The output of the controller is the reference voltage for the LC. It is a proportional resonant (PR) controller based on [14] which

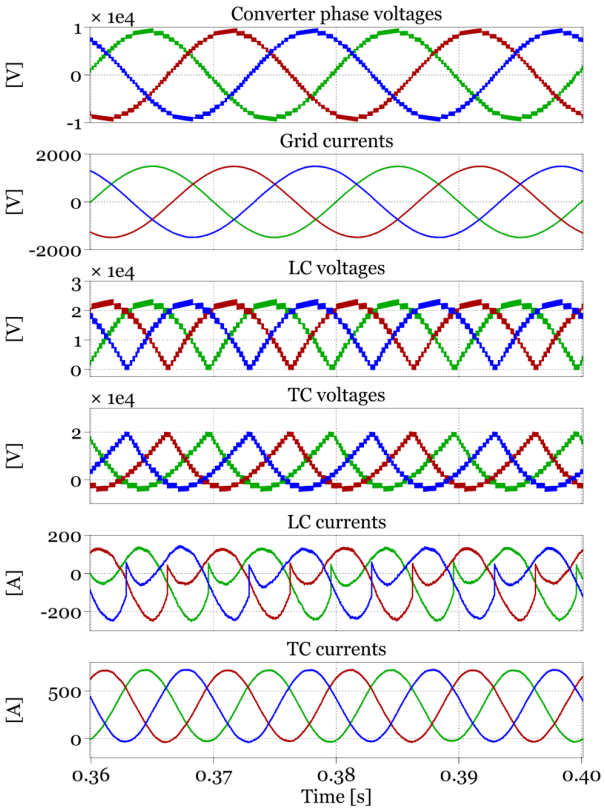

Fig. 5. Simulation waveforms in normal operation at 20 MW with PF = 1

derives PR controller structure and coefficients according to desired transient behavior of the AC signal amplitude [14]. Unlike previous control loops, the AC current loop is designed to control all three phases at the same time. A block diagram for this loop is shown in Figure 4.

VII. Simulation Results

A simulation model of the PCUB has been implemented in PLECS to validate the operation of the converter. Simulation parameters are presented in Table II.

TABLE II
Simulation Parameters

Parameter	***Value***
Active Power P	20 MW
Reactive Power Q	8 MVAr
AC Voltage V_{l-l}	11 kV
DC voltage	20 kV
Turn ratio r	2.44
Nominal cell voltage V_{sm}	1.5 kV
Cell capacitance LC	1.9 mF
Cell capacitance TC	0.8 mF
Number of cells (LC+TC)	15 + 15

The required number of cells is calculated based on the peak-peak voltage pulsation in the chainlinks for the optimised turn ratio. The model has been built using 15 half-bridges in the LC and 15 full-bridges in the TC assuming a nominal cell voltage of 1.5 kV. Cell capacitance values are taken from the

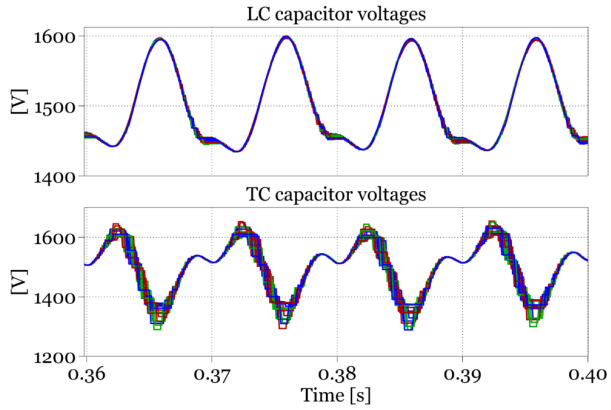

Fig. 6. Capacitor voltages for phase *a* under normal operation at 20 MW with PF = 1

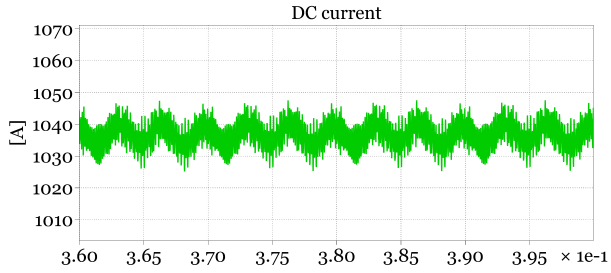

Fig. 7. DC current

results of the turn ratio analysis. A level-shifted PWM based modulation scheme has been used to modulate the converters and a simple sorting algorithm is employed to balance the capacitor voltages.

Simulation waveforms are presented in Figures 5 - 7. Steady-state waveforms of the AC side and CL voltages and currents are presented in Figure 5 under balanced grid conditions. From Figure 6, it can be seen that the ripple in the capacitor voltages is within the 20 % margin when the cell capacitors are chosen based on the optimised turn ratio. In Figure 7, it can be observed that the 2ω balancing currents in the phases do not appear in the DC current. However, a small 6th harmonic ripple can be observed. It is because due to minor inaccuracies in the harmonic cancellation between the LC and the TC, the circulating current through the arms have small unwanted even harmonics (in addition to the large injected 2nd). These unwanted even harmonics all cancel out on the DC side since they are all either positive or negative sequence except the zero sequence 'even triplens', out of which only the 6th is big enough to appear in the DC current. If required, this 6th harmonic in the DC current can be suppressed by introducing a slight variation in the control that uses a resonant control loop on the circulating current in the phases.

VIII. Conclusion

A new hybrid multilevel VSC converter, named PCUB, has been introduced in this paper to improve performances of hybrid converters while keeping low energy storage requirements. A description of the converter topology, basic mathematical analysis and a control scheme for the converter has been presented in balanced grid conditions. The PCUB's operation has been optimised by operating at an optimum turn ratio value that results in the lowest energy requirements in the CLs. Results from a 20kV DC - 11kV AC and 20MW PLECS simulation model have been shown to demonstrate the operation of the converter. The PCUB is shown to have a much smaller footprint than the MMC owing to the 6-7 times smaller energy storage.

References

[1] N. Hingorani, "High-voltage DC transmission: a power electronics workhorse", IEEE Spectrum, vol. 33, no. 4, pp. 63-72, 1996.
[2] B.R. Andersen, L. Xu, P.J. Horton, P. Cartwright. Topologies for VSC transmission, Power Engineering Journal, 16(3), pp. 142-150, (2002).
[3] J Dorn, H Huang, and D Retzmann. Novel voltage sourced converters for hvdc and facts applications, Conference proceeding CIGRE - Osaka, 314, (2007).
[4] O. Oni, I. Davidson and K. Mbangula, "A review of LCC-HVDC and VSC-HVDC technologies and applications", 2016 IEEE 16th International Conference on Environment and Electrical Engineering (EEEIC), 2016.
[5] H. Alyami and Y. Mohamed, "Review and development of MMC employed in VSC-HVDC systems," 2017 IEEE 30th Canadian Conference on Electrical and Computer Engineering (CCECE), Windsor, ON, 2017, pp. 1-6.
[6] M. Barnes and A. Beddard, "Voltage Source Converter HVDC Links The State of the Art and Issues Going Forward", Energy Procedia, vol. 24, pp. 108-122, 2012.
[7] C. Oates, "Modular Multilevel Converter Design for VSC HVDC Applications", IEEE Journal of Emerging and Selected Topics in Power Electronics, vol. 3, no. 2, pp. 505-515, 2015.
[8] R. Marquardt, "Modular Multilevel Converter topologies with DC-Short circuit current limitation", 8th International Conference on Power Electronics - ECCE Asia, 2011.
[9] S. Debnath, J. Qin, B. Bahrani, M. Saeedifard and P. Barbosa, "Operation, Control, and Applications of the Modular Multilevel Converter: A Review", IEEE Transactions on Power Electronics, vol. 30, no. 1, pp. 37-53, 2015.
[10] J. Wang, R. Burgos and D. Boroyevich, "A survey on the modular multilevel converters; Modeling, modulation and controls", IEEE Energy Conversion Congress and Exposition, 2013.
[11] M. M. C. Merlin et al., "The Alternate Arm Converter: A New Hybrid Multilevel Converter With DC-Fault Blocking Capability," in IEEE Transactions on Power Delivery, vol. 29, no. 1, pp. 310-317, Feb. 2014.
[12] H. Wickramasinghe, G. Konstantinou, J. Pou, R. Picas, S. Ceballos and V. Agelidis, "Comparison of bipolar sub-modules for the alternate arm converter", IECON 2016 - 42nd Annual Conference of the IEEE Industrial Electronics Society, 2016.
[13] E. Amankwah, A. Costabeber, A. Watson, D. Trainer, O. Jasim, J. Chivite-Zabalza, and J. Clare, The series bridge converter (SBC): Design of a compact modular multilevel converter for grid applications, in IECON 2016 - 42nd Annual Conference of the IEEE Industrial Electronics Society, Oct 2016, pp. 25882593.
[14] A. Kuperman, "Proportional-Resonant Current Controllers Design Based on Desired Transient Performance," in IEEE Transactions on Power Electronics, vol. 30, no. 10, pp. 5341-5345, Oct. 2015.
[15] H. Fujita, S. Tominaga, and H. Akagi, Analysis and design of a dc voltagecontrolled static var compensator using quad-series voltage-source inverters, IEEE Trans. Ind. Appl., vol. 32, no. 4, pp. 970977, Jul./Aug. 1996.
[16] H. Akagi, "Classification, Terminology, and Application of the Modular Multilevel Cascade Converter (MMCC)," in IEEE Transactions on Power Electronics, vol. 26, no. 11, pp. 3119-3130, Nov. 2011.
[17] M. Hagiwara, R. Maeda and H. Akagi, "Control and Analysis of the Modular Multilevel Cascade Converter Based on Double-Star Chopper-Cells (MMCC-DSCC)," in IEEE Transactions on Power Electronics, vol. 26, no. 6, pp. 1649-1658, June 2011.